

# Seismological Research at Georg-von-Neumayer Base, Antarctica

## Part I: The Seismological Observatory

By Jan Wüster \*, Alfons Eckstaller\*\* and Heinz Miller \*\*

**Summary:** Since 1982 seismological observations are continuously carried out at the German Georg-von-Neumayer base (GvN), Antarctica. The special situation, the station is located on a floating ice shelf, results in some reductions concerning the quality of the data. On the other hand these site-caused disadvantages enable a number of special investigations, like the analysis of icequakes, the dispersion of flexural waves within the ice-shelf or the transmission of vertically polarized S-waves. Beside the geophysical observatory itself, a network of several remote stations is also operated. This network allows, within some limits, the determination of apparent velocities and azimuths so that for nearer teleseismic events a sufficient accurate localisation of earthquakes can be realized. Thereby it could be shown that ISC-locations of earthquakes in the South Sandwich Islands area are probably systematically biased. Some earthquakes within the Antarctic continent could also be detected. Furthermore the observations allow certain conclusions to be drawn about the structure of the deeper earth below the area of the GvN-station.

**Zusammenfassung:** Seit 1982 werden an der deutschen Georg-von-Neumayer Station (GvN) kontinuierlich seismologische Beobachtungen durchgeführt. Bedingt durch die Lage der Station auf einer schwimmenden Schelfeisplatte gibt es einige Einschränkungen bezüglich der Datenqualität. Diese standortbedingten Nachteile erlauben jedoch andererseits eine Reihe von speziellen Untersuchungen wie der Analyse von Eisbeben, der Dispersion von Plattenbiegewellen in der Eisplatte oder der Transmission von vertikal polarisierten S-Wellen. Neben dem eigentlichen geophysikalischen Observatorium wird auch ein Netz von mehreren entfernteren Außenstationen betrieben. Das Netzwerk ermöglicht in bestimmten Grenzen die Bestimmung von Scheingeschwindigkeiten und Azimuten, so daß auch bei näheren teleseismischen Ereignissen eine hinreichend genaue Lokalisierung von Erdbeben durchgeführt werden kann. Dabei konnte gezeigt werden, daß ISC-Lokalisierungen von Beben im Bereich der South Sandwich Inseln sehr wahrscheinlich einen systematischen Fehler aufweisen. Es konnten auch einige Beben innerhalb der Antarktis beobachtet werden. Des weiteren ermöglichen die Beobachtungen auch einige Rückschlüsse auf die Struktur des tieferen Untergrundes im Bereich der GvN-Station.

### INTRODUCTION

When seismological observations at the German Antarctic base "Georg von Neumayer" (GvN, 70°37' S, 80°22' W, station code VNA) commenced in 1982, achievable data quality was uncertain because the station is situated on a floating ice shelf. Nevertheless certain research goals were formulated (MILLER & ECKSTALLER 1982). Apart from contributing to the international network of seismographic stations, data from GvN could be used in special studies on:

- focal mechanisms of icequakes,
- local seismicity and tectonic earthquakes,
- structure of the earth's crust through determination of travel time residuals and slowness anomalies,

- structure of crust and upper mantle through absorption spectra of teleseismic events,
- surface waves,
- movements of the ice-shelf induced by ocean and atmosphere.

Ice-shelf movements at tidal frequencies were analyzed using gravimeter and tiltmeter data. These results have been published earlier (KOBARG & LIPPMANN 1986). At seismic frequencies the ice shelf was found to be extremely susceptible to the induction of long-period flexural waves and eigenmodes of vibration, rendering long-period seismometry futile and precluding studies on surface waves. In this first paper of two we will summarize observation procedures, the local network of stations and some results to be deduced for the more local vicinity.

### SEISMOLOGY ON A FLOATING ICE-SHELF

From a seismological point of view an ice-shelf must be considered an unfavourable location. An ice shelf is an ice sheet of variable thickness floating on a water layer. Thus at an ice shelf site no direct observation of transversal (S) waves is possible since they cannot be transmitted through this water layer. Theoretically one might expect the occurrence of SV/P-conversion (the conversion of vertically polarized S-phases into longitudinal (P) waves) at the seafloor. This conversion of energy will depend on the velocity contrast and the angle of incidence. From Figure 1 40% transmission should be expected for epicentral distances  $\Delta < 20^\circ$  in case of an acoustically hard sea floor. In fact, only few and very weak S-phases are observed, which moreover appear to enter the ice at an ice rumple near network station EB, where the ice-sheet makes contact with a local high in the sea floor. With S-phases lacking, the standard method for calculating epicentral distance from the travel time difference S-P cannot be used, nor can earthquake magnitudes be easily estimated.

The water layer not only reflects transverse waves but acts as a kind of resonance chamber for longitudinal waves (Fig. 2.) For this reason the main frequency content in seismograms depends on the properties of the oscillating system, comprising sea floor, water layer and ice-shelf, more than on properties of the earthquake source or the path travelled by the waves. On unfiltered tracks, the first onset appears like a high-frequency precursor to a low-frequency signal and is often hard to detect with certainty. The effect has been modelled using synthetic seismo-

\* Dipl.-Geophys. Jan Wüster, Institut für Geophysik, Ruhr-Universität Bochum, Postfach 10 21 48, D-W-4630 Bochum, FRG.

\*\* Dr. Alfons Eckstaller and Prof. Dr. Heinz Miller, Alfred Wegener Institute for Polar and Marine Research, Columbusstrasse, D-27515 Bremerhaven, FRG.  
Manuscript received 10 January 1992; accepted 23 July 1992.

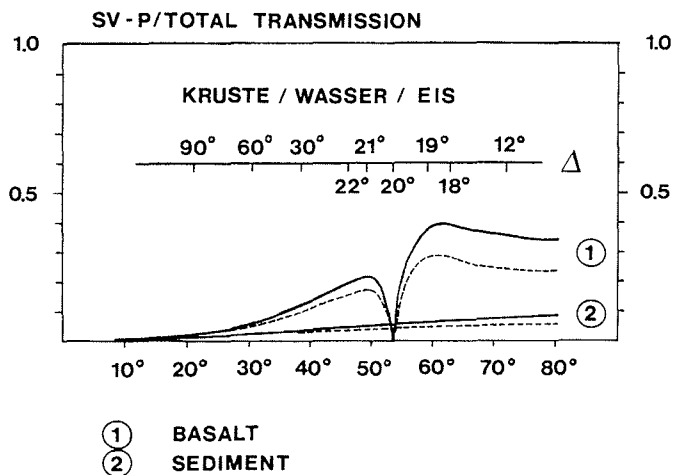


Fig.1: Relationship  $T_{sv-P(i)}$  between coefficient of transmission  $T$  and angle of incidence  $i$  for 3 layers (crust, water, ice). The corresponding epicentral distance is plotted above. Model (1), sea-floor = basalt, displays a critical angle at  $\Delta = 20^\circ$ . For closer epicenters, approx. 40% of vertically polarized S-energy is converted to P waves and transmitted. Model (2), sea-floor = sediment, shows very little conversion for any epicentral distance.

Abb. 1: Beziehung  $T_{sv-P(i)}$  zwischen dem Transmissionskoeffizienten  $T$  und dem Einfallswinkel  $i$  für 3 Schichten (Kruste, Wasser, Eis). Die entsprechenden Epizentralabstände sind auf der darüberliegenden Skala abgetragen. Modell (1): Meeresboden = Basalt, zeigt einen kritischen Winkel bei  $\Delta = 20^\circ$ . Für nähere Epizentren wird ca. 40% der vertikal polarisierten S-Wellen-Energie in P-Wellen umgewandelt und transmittiert. Modell (2): Meeresboden = Sediment, zeigt für beliebige Epizentralabstände nur geringe Konversion.

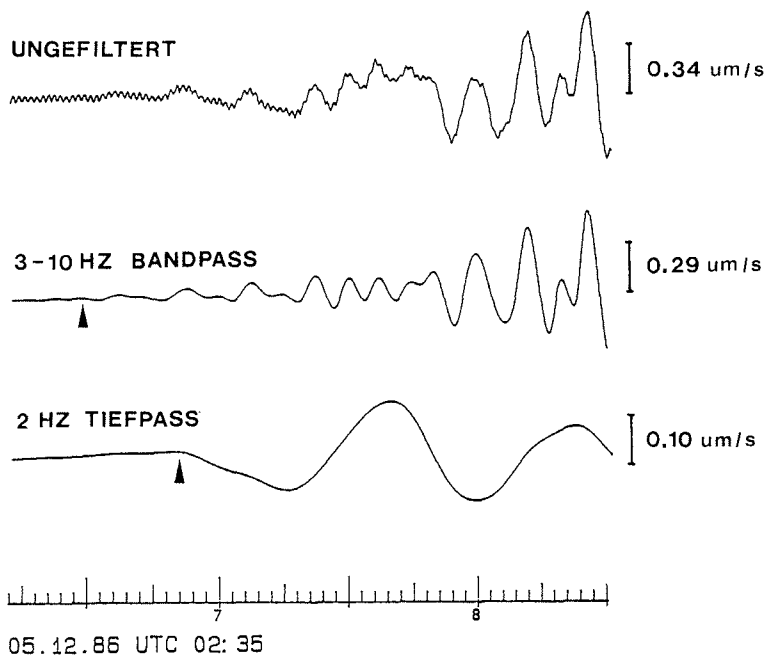


Fig. 2: First onset at station OBS, EW-component of an event in the South-Sandwich Islands region, hypocentre according to ISC 05.12.86, UTC 02:31:55.8, located at  $\phi = 59.0^\circ$  S,  $\lambda = 25.3^\circ$  W,  $z = 82$  km,  $m_b = 4.9$ .

Track 1 represents the unfiltered seismogram. An expected impulsive onset of a high-frequency signal as marked by an arrow on track 2 (digitally filtered with a band-pass filter 3-10 Hz) appears strongly damped. Its energy is diverted into low-frequency resonance modes brought out by the low-pass filter in track 3.

Abb. 2: Ersteinsatz eines Bebens im Gebiet der South Sandwich Inseln an der EW-Komponente der Station OBS. Herdparameter nach ISC: 05.12.86 UTC 02:31:55.8, lokalisiert bei  $\phi = 59.0^\circ$  S,  $\lambda = 25.3^\circ$  W,  $z = 82$  km,  $m_b = 4.9$ .

Spur 1 zeigt das ungefilterte Seismogramm. Ein Pfeil markiert auf Spur 2 (digital bandpaßgefiltert von 3-10 Hz) den eigentlich impulsiven Einsatz eines hochfrequenten Signalanteiles. Dieser erscheint stark gedämpft, seine Energie speist tieffrequente Resonanzmoden, die durch den Tiefpaßfilter in Spur 3 deutlich herausgebracht werden.

grams and has been checked by some test explosions. Strong pulses can generate flexural waves travelling horizontally along the ice-shelf. These wave trains have also been observed on the Ross ice-shelf (HATHERTON 1961). These waves are highly dispersive, their dispersion relation is a function of the thickness of the ice. Observed dispersion is in good agreement with calculations using ice thicknesses determined by EMR-measurements. A typical group velocity is 0.63 km/s at 0.5 Hz and amplitudes grow towards lower frequencies (up to 2 mm at 0.05 Hz), creating a continuous red noise spectrum.

Ground noise causes severe limitations in data quality. While Miller et al. (1983) found a maximum noise level of 10 nm/s at the foot of nunatak Passat 150 km to the south-east of the base, the noise level on the shelf-ice is at least 500 nm/s under favourable conditions (i.e. ice covered sea, little wind and no incoming tide). During Antarctic summer the swell of the open sea often induces eigenvibrations of the ice-sheet with periods of 15 - 20 s, and in all seasons strong winds generate high-frequency noise on the rough surface of the ice. The limiting wind velocity is about 15 m/s, above which seismic signals cannot be recorded properly. This is in agreement with IKAMI & ITO (1984) reporting the same value from the East-Antarctic inland ice. Even if digital filtering could recover a signal from very strong noise, the trigger algorithms do not work and cannot activate digital recording under these conditions. Gaps in the data result.

Sometimes the most prominent feature is a horizontal impulsive onset repeated in characteristic intervals (Fig. 8). The occurrence of this phenomenon is correlated with the tidal current and was identified as ice-floes afloat in neighbouring Atka-bay which are colliding with the ice-shelf in the rhythm of the swell (Fig. 9).

Apart from distorting or blocking earthquake signals, the ice-shelf is an active source of numerous icequakes. Various, not mutually exclusive hypotheses exist about their origins:

- slip-stick movements of the ice over its supporting base (i.e. the ice-rumples);
- formation of cracks due to excessive strain rates,
- fatigue failure of the ice-shelf, after the material has been thoroughly exhausted by tidal flexing;
- tensile fractures at the ice edge and further opening of inlets due to divergent deformation of the ice-shelf.

Seismic waves originating from icequakes cannot leave the ice because of total reflection at the ice/water interface, nor can they propagate along straight lines because of a strong velocity gradient within the ice (MÜHLSTEIN 1991). They therefore produce characteristic seismograms with soft onsets and pronounced dispersion. Thus icequakes can easily be distinguished from tectonic earthquakes (Fig. 3).

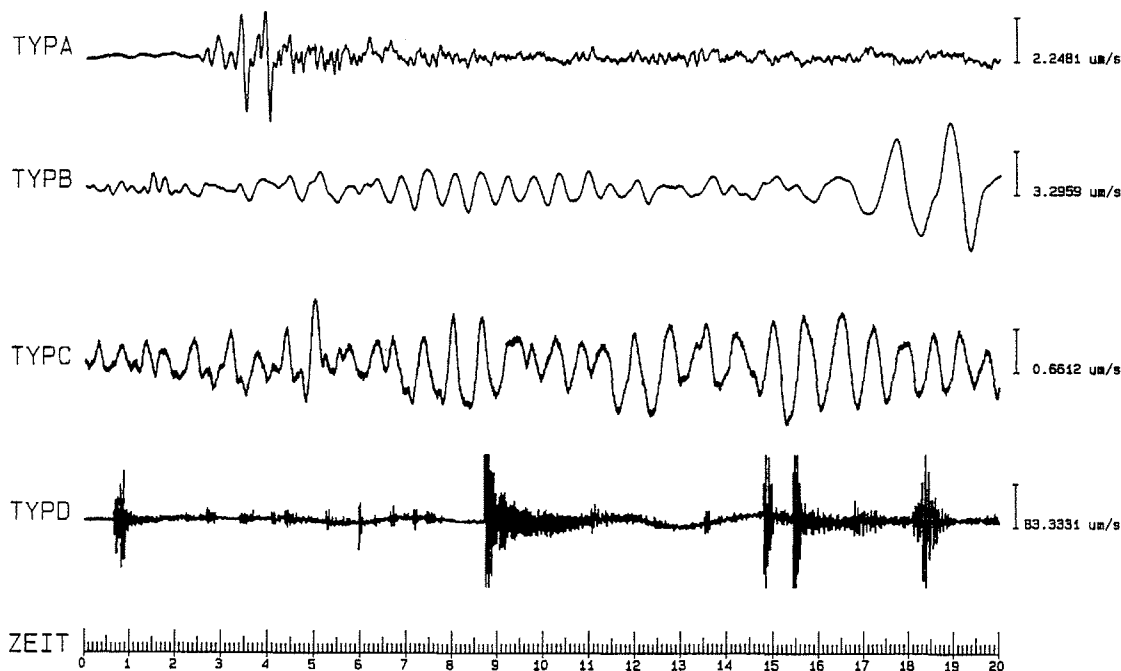


Fig. 3: Types of icequakes observed on Ekström ice-shelf.

Type A: relatively close event, can usually be located, S-onset visible. Type B: distant event, dispersion has seriously distorted the wave train. Type C: continuous vibration, can go on for minutes, not an event in the seismo-logical sense of the word. Type D: micro-cracks exclusively observed at network station EB, resembling snow-cracks described in Nishio (1983).

Abb. 3: Auf dem Ekström-Schelfeis beobachtete Eisbeben typen.

Typ A: relativ nahes Ereignis, kann für gewöhnlich lokalisiert werden, S-Einsatz sichtbar. Typ B: fernes Ereignis, Dispersion hat den Wellenzug stark deformiert. Typ C: andauernde Schwingung, kann minutenlang anhalten, kein Ereignis im Sinne der Seismologie. Typ D: Mikrobeben, die ausschließlich an der Außenstation EB beobachtet werden. Sie ähneln sog. „snowcracks“, die von Nishio (1983) beschrieben werden.

Further inconveniences include the drift of the ice (approx. 150 m/a towards the North) enforcing yearly redetermination of station positions, instrumental malfunctioning of network stations in severe storms and drainage of their batteries at low temperatures, sometimes reducing the number of active stations to one. Recent experiments with local power supply by windgenerators have been successful.

## DATA ACQUISITION

The disadvantages of GvN as a seismological station mentioned above are partly compensated by the existence of a small seismic network around the central observatory (Fig. 4). At times special small-scale arrays have existed north of GvN for specialized icequake studies (v. d. OSTEN-WOLDENBURG 1990, NIXDORF 1992). Positions of remote stations have varied over the years. They had to be chosen according to accessibility rather than for optimum array shape. Generally, with growing experience, baselines were extended and stations WEST (WS) and SOUTH (SS) gradually pushed outwards. A location on sea ice over the frozen Atka Bay was given up after 1983, establishing instead station EB near the rugged ice rumple in the north-west. Station OT was established 60 km to the south (but still north of the grounding line, above water) in 1985, at the end of 1987 it was moved onto the top of the ice rise Sørraasen 80 km southeast of GvN for better radio contact and avoidance of S-wave reflection and resonances in the water. And finally, one year later station EB, which had predominantly registered icequakes and microcracks, was moved to the Halfvar ridge about 50 km to the southeast. Exact positions of seismograph stations up to wintering season 1986/87 are listed in Wüster (1989). The sketchmap (Fig. 4) shows the present situation.

The central observatory (OBS) is located 1 km south of GvN base in a cavern in the firm (for details see MILLER & ECKSTALLER 1982). It is equipped with 3-component GEOTECH S13 seismometers set to 1 Hz eigenfrequency.

Data from all seismometers are transmitted to the base, where they are recorded digitally in event triggered mode. Data from the remote locations are transmitted using RF-telemetry links, the observatory is linked by cable. For recording signals were initially band limited to 50 Hz and at a later stage, when the highest observed frequencies became known, this was reduced to 30 Hz. The trigger algorithm used is a short term/long term averager with a number of parameters such as prefiltering, threshold, trigger length and coincidence between selectable channels. A pre-event memory enables full waveform recording. In order to obtain a full record of events a monitor record of the 3-component OBS station is written on an ink recorder. This monitor record is used for picking arrival times; for events of interest the digitally recorded data can be played out in analog form at various gain settings. For further analysis digital data can be read into the observatory's computing facilities (PDP 11).

With time, research interests shifted from icequakes and other

ice-sheet related phenomena to studies involving hypocenters at teleseismic and intermediate distances, as reflected by the reduction in sampling frequency, the extension of baselines and the quest for quiet station sites. The following changes and improvements are envisioned for the near future:

- The old PCM recording system should be replaced by a gain ranging system with a dynamic range of 140 dB. Signal transmission will be fully digital in order to preserve dynamic range.
- The short period seismometers, especially the 3-component seismometers, will be fitted with electronic feedback circuitry to extend sensitivity to periods of 15 to 20 s.
- New power supplies making use of wind and solar energy should guarantee long operating periods without power failures
- One or two remote stations will be installed far south of the base, to achieve a better coverage of the Ekström ice-shelf area.

## DATA ANALYSIS

Standard processing at Bremerhaven begins with a playback of the digital recordings. Data from each seismometer are grouped by events and stored on ANSII standard tapes. At the same time analog plots are produced, to identify noise-triggered recordings, to divide events roughly into the groups teleseisms, intermediary-distance events and local events and to select promising events for further processing. The analog plots allow onsets to be read to an accuracy of 0.1 s. As seen on Figure 5, GvN can detect teleseisms from the whole southern hemisphere. Under low noise conditions (see above) the detection threshold lies at magnitude  $m_b = 4.4$  at  $10^\circ$  and  $m_b = 4.6$  at  $100^\circ$  epicentral distance.

Original recordings of selected events can now have their dc-offsets removed, they can be de-spiked and arbitrarily filtered using standard methods of discrete time-series analysis. Plots with high resolution in time and amplitude allow more accurate readings of phases, signal amplitudes and frequencies, which then form the basis of further investigation.

Localization of icequakes (type A, Fig. 3) has been carried out with iterative improvement of hypocenter coordinates by the method of least squares (FASTHYPO). ECKSTALLER (1988) used a single-layer-model of the ice-shelf with P and S wave velocities of 3.3 and 1.9 km/s. A model with 9 layers has also been used (v. d. OSTEN-WOLDENBURG 1990). Figure 6 shows that some epicenters are located in the sea. This is a drastic reminder that our simple assumptions about propagation of seismic waves in the ice-sheet do not hold. Deviations must be expected in the near or intermediate field of a complex radiation pattern within a roughly plane-parallel suspended plate, heavily crevassed, the thickness of which is of the order of wavelengths involved and which contains a steep gradient of velocity with depth! Current investigations (NIXDORF 1992) are concerned with both focal mechanisms and wave propagation of

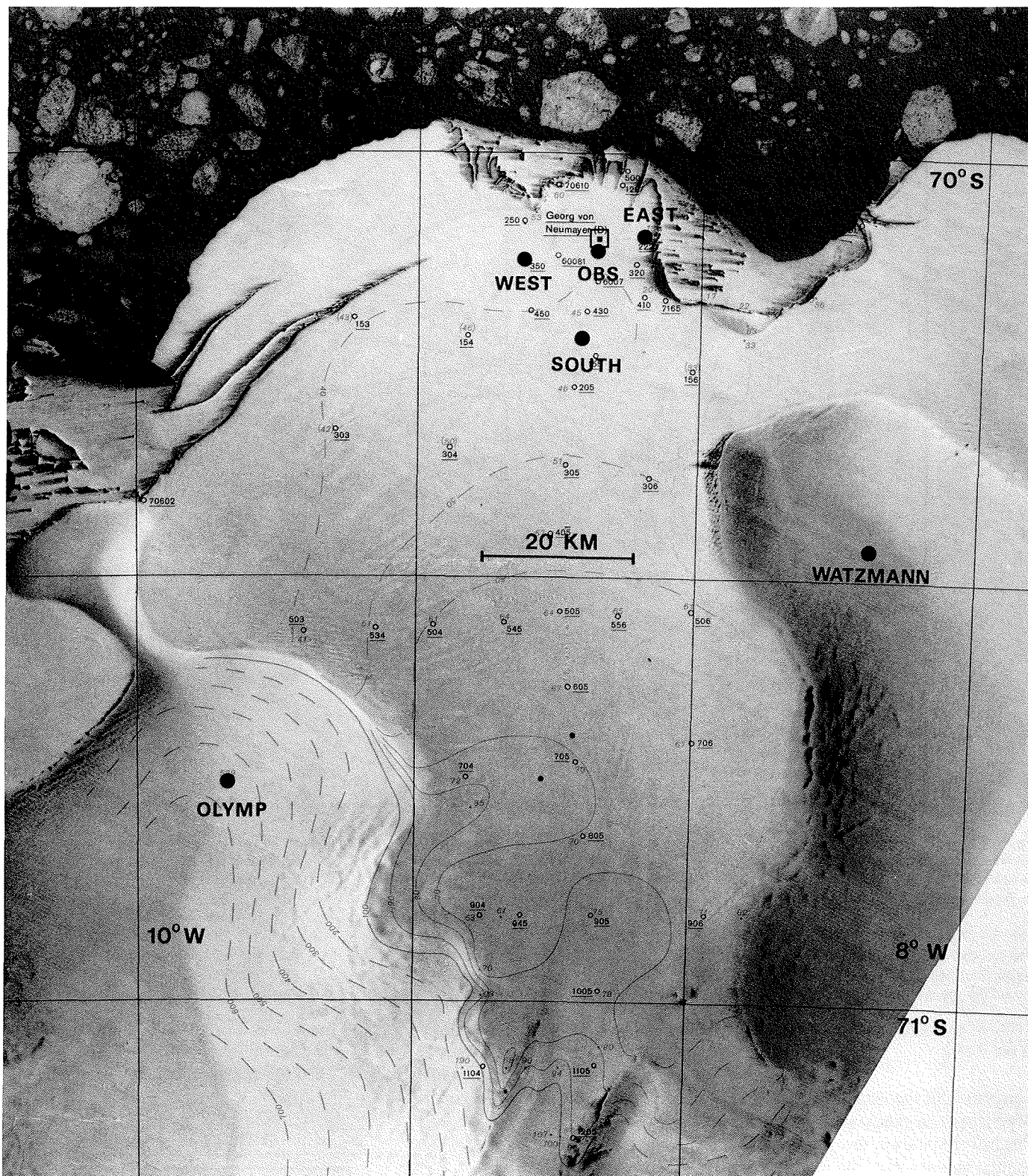


**Fig. 4:** The map sketch, based on a satellite photograph, shows the state of the GvN network of seismic stations during wintering season 1990/91. Seismic stations are depicted by black dots. GvN base is located 1 km north of station OBS. Exact positions for pre-1987 seasons are given in Wüster (1989). Note that stations OLYMP and WATZMANN are situated on the ice-rises Søråasen and Halfvar, resp., approx. 500 m above sea level, where the ice shelf rests on solid ground. The station EB mentioned in the text was dismantled in 1988. Its position was to the NW of the base, near the point labeled 70610 on the map.

**Abb. 4:** Die Kartenskizze basiert auf einem Satellitenfoto und zeigt den Zustand des seismischen Netzes um GvN während der Überwinterung 1990/91. Die seismischen Stationen sind durch schwarze Punkte gekennzeichnet. Die GvN-Station liegt 1 km nördlich der Station OBS. Die genauen Koordinaten aller Netzstationen für die Zeit vor 1987 sind von Wüster (1989) veröffentlicht. Die Stationen OLYMP und WATZMANN stehen auf den Eisrücken Søråasen und Halfvar in etwa 500 m Höhe über NN, dort liegt das Eis auf festem Untergrund. Die im Text erwähnte Station EB wurde 1988 abgebaut. Ihre Position war nordwestlich von GvN nahe dem Punkt 70610.

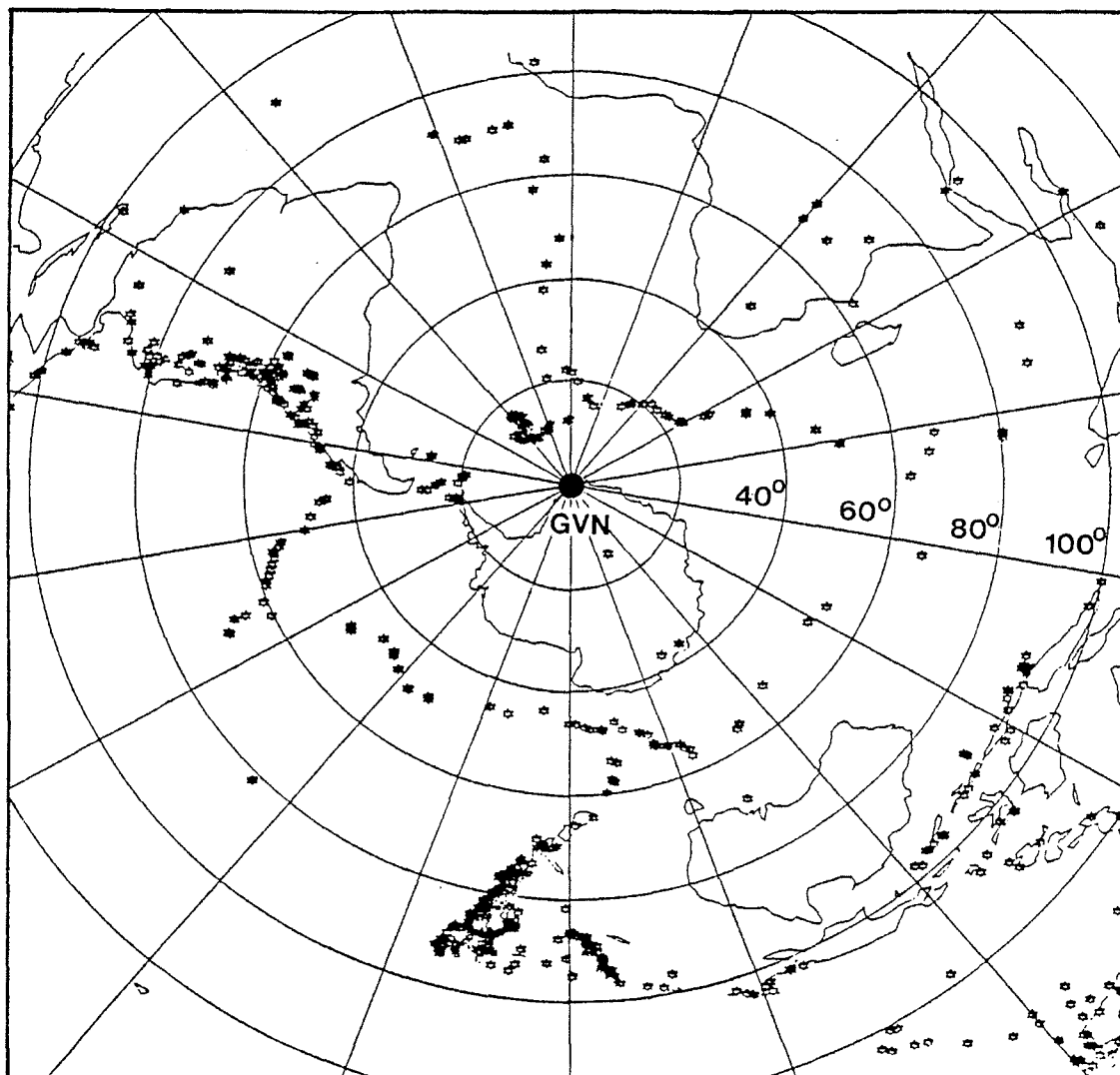


**Fig. 5:** Geographical distribution of epicenters of events registered at GvN from 1982 to 1984 (azimuthal equidistant projection with GvN at its center.) Epicenters were taken from ISC-Bulletin. The nearest seismically active area is the South Sandwich deep sea trench and island arc, at about 1500 km to the NW. GvN is the seismological station closest to this area. Other important source regions are Fidschi-Tonga-Kermadec region on the opposite side of the Antarctic continent and the Andes region in South America.

**Abb. 5:** Geographische Verteilung der an GvN von 1982 bis 1984 registrierten Beben (azimutal-äquidistante Projektion mit GvN als Mittelpunkt). Die Epizentren sind den ISC-Bulletins entnommen. Das nächstgelegene seismisch aktive Gebiet ist der South Sandwich Tiefseegraben mit zugehörigem Inselbogen, etwa 1500 km nordwestlich. GvN ist für dieses Herdgebiet die nächste, regelmäßig meldende Station. Das zweitwichtigste Herdgebiet ist die Region Fidschi-Tonga-Kermadec auf der gegenüberliegenden Seite des antarktischen Kontinents. An dritter Stelle steht die Andenregion in Südamerika.

icequakes originating near an inlet at the ice edge to the north of the base.

Correlation of the frequency of icequake-occurrence with gravity values constantly measured in the observatory at GvN has conclusively shown, that most icequakes are triggered by tidal vertical movement of the ice-shelf (KOBARG & LIPPMANN 1986, ECKSTALLER 1988).

Teleseismic hypocenters cannot be located by a small seismic network. But if determination of two parameters (focal time and depth) are dropped, angles of back-azimuth and incidence of the incoming quasi-plane wave fronts can be determined, if a minimum of three arrival times at non-collinear stations or amplitudes of first onsets on at least one 3-component-stations are available.

The most successful method as a first step computes apparent velocities  $v_a$  and  $v_b$  of the first P-onset along two measuring lines a and b (Fig. 7). Then the apparent velocity along the surface is

$$v_s = \frac{\sin \alpha}{\sqrt{\frac{1}{v_a^2} + \frac{1}{v_b^2} - \frac{2}{v_a v_b} \cos \alpha}}$$

Angles  $\varphi_a$  and  $\varphi_b$  and thus the azimuth angle of the incoming wavefront with respect to lines a and b are

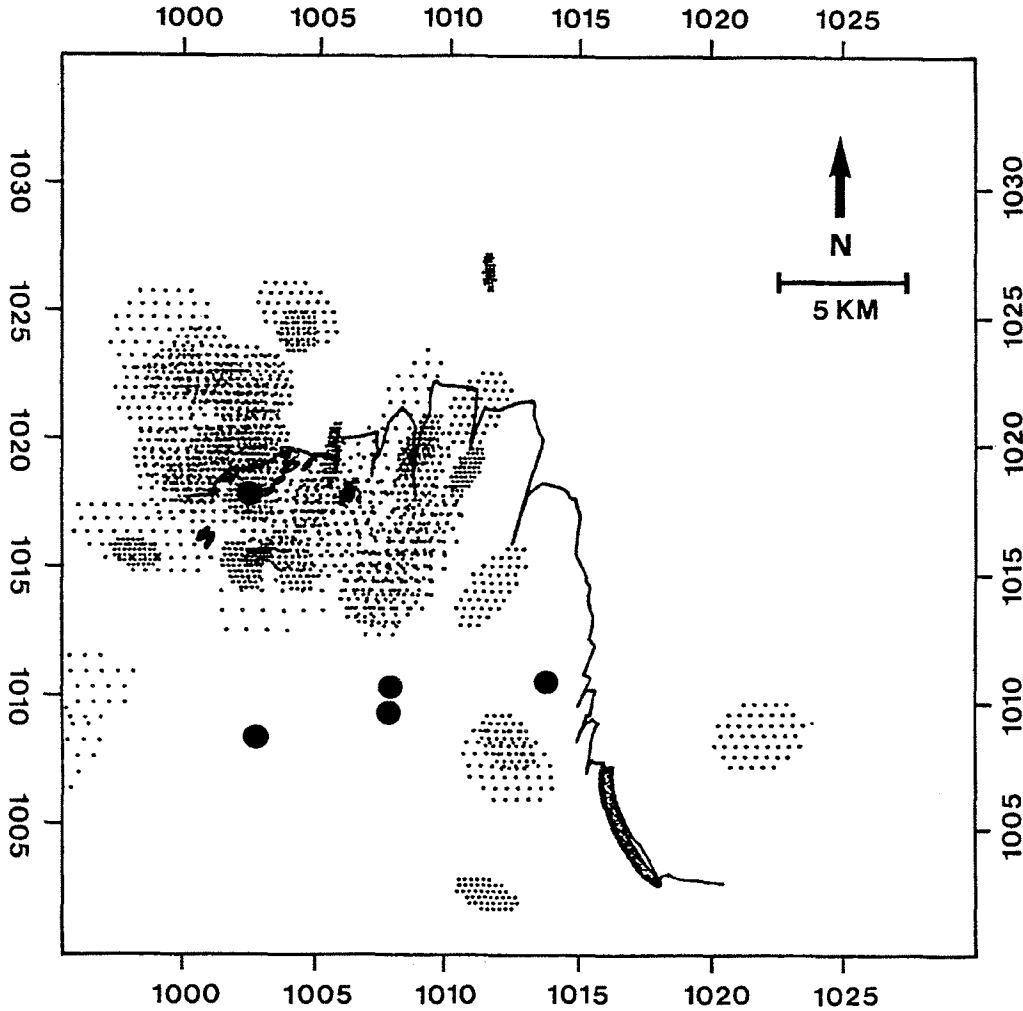


**Figure 6:** Icequakes located in the vicinity of GvN base from April to October 1984. Big black dots indicate the positions of seismic stations at that time. Small dots indicate error ellipses of icequake epicenters located by FASTHYPO. Most of the seismicity is found along the ice edge to the N and NW of the base. Hypotheses about its causes are presented in the text. Note that a considerable amount of epicenters is located in the sea. Apart from poor resolution for out-of-network events this indicates, that wave propagation in the ice-sheet was not modelled adequately.

**Abb. 6:** In der Nähe von GvN von April bis Oktober 1984 lokalisierte Eisbeben. Die dicken schwarzen Punkte symbolisieren die Positionen seismischer Stationen zu dieser Zeit. Die kleinen Pünktchen stehen für die Fehlerellipsen der mit FASTHYPO lokalisierten Eisbeben-Epizentren. Entlang der Eiskante im N und NW der GvN-Station ist die Seismizität am stärksten. Hypothesen über ihre Ursachen werden im Text angeführt. Man beachte, daß nicht wenige Epizentren im Meer lokalisiert wurden. Abgesehen von der geringen Lokalisierungsgenauigkeit für außerhalb des Netzes gelegenen Ereignissen zeigt sich hier auch, daß die Wellenausbreitung im Schelfeis nicht gut genug modelliert worden ist.

$$\varphi_a = \arccos\left(\frac{v_s}{v_a}\right), \quad \varphi_b = \arccos\left(\frac{v_s}{v_b}\right)$$

If measurements along more than two azimuths can be obtained and arrival times are subject to random or systematic measurement error, several different values for  $v_{app}$  are obtained, the average  $v_{app}$  of which is the best estimate for the apparent velocity along the surface. Efforts to minimize its standard error by slightly adjusting observed arrival times within certain error limits lead to a kind of regression analysis. This procedure, when applied to a significant number of events, may even be used for the determination of travel-time residuals at individual network stations and the subsequent allotment of station correction terms to counteract them.

The inverse of the absolute value of  $v_{app}$  is the slowness  $S = dT/d\Delta$  (with travel-time  $T$  and epicentral distance  $\Delta$ ) which can be read from travel-time tables, determination of  $v_{app}$  theoretically also yields  $D$ . In practice, however, the accuracy attained permits rough classification of epicentral distance only. Likewise, the angle of incidence is related to  $S$ , so the 3-component stations give an independent estimate of epicentral distance as well as azimuth.

Azimuth angles determined by the procedures described above agree with calculated angles in case of known hypocenters within an error margin of  $\pm 5^\circ$ .

Teleseismic travel time residuals form the basis for investigations on the structure of the earth's crust and upper mantle be-

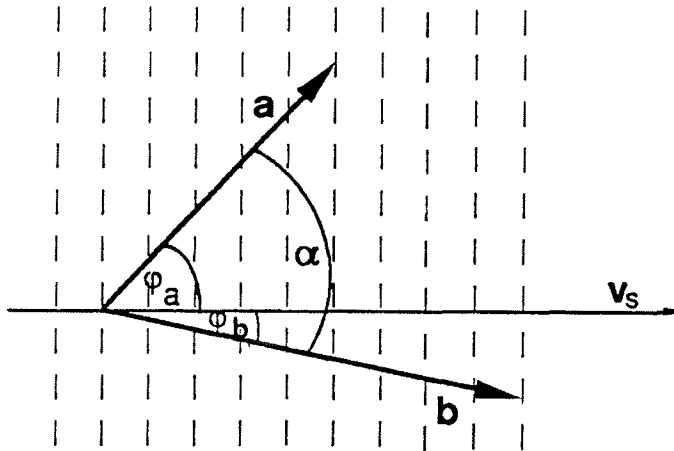


Fig. 7: Calculation of apparent velocity of a plane wave propagating across the network. Wavefronts (i.e. surfaces of equal phase) are indicated by dashed lines. Two measuring lines  $\underline{a}$  and  $\underline{b}$  are imagined between two network stations each; they may always be parallel-shifted to a common origin, because the wavefronts are parallel and even. The projection of their wave vector onto the earth's surface is  $\underline{v}_{app}$ , the vector of apparent velocity.

Abb. 7: Berechnung der Scheingeschwindigkeit einer ebenen Welle, die das Netzwerk durchläuft. Wellenfronten (d.h. Flächen gleicher Phase) sind durch gestrichelte Linien gekennzeichnet. Zwischen je zwei Netzstationen stellt man sich die Meßstrecken  $\underline{a}$  und  $\underline{b}$  vor; sie lassen sich stets an einem gemeinsamen Punkt parallel verschieben, da die Wellenfronten parallel und eben sind. Die Projektion des Wellenvektors auf die Erdoberfläche ist  $\underline{v}_{app}$ , der Vektor der Scheingeschwindigkeit.

neath Queen Maud coast. These investigations will be described in detail in part II of this paper.

## RESULTS

### 1. ISC-locations of South-Sandwich events are probably biased

Extremely high absolute negative travel time residuals (up to -10 s) observed at GvN for the epicentral area closest to GvN (South Sandwich Island Region) had nurtured suspicion that hypocentral locations in this area are systematically inaccurate. An earthquake sequence which occurred on January 30/31 1987 southeast of this island arc provided an opportunity to investigate this in detail. 29 shocks were digitally recorded at GvN, 16 of which appear in the ISC-Bulletin and only one of those was missed by the trigger. The main shock occurred at 22:29:43 UTC, at location  $\phi = 60.05^\circ$  S,  $\lambda = 26.88^\circ$  W, with  $z = 53$  km, and reached a magnitude  $m_b = 6.0$ . Aftershocks lasted for 21 hours (Fig. 8). Within error limits they all originated from the same hypocenter, so that travel-times could be averaged, giving a negative travel-time residual of  $-6.1 \pm 1.7$  s.

Other seismographic stations on the coast of Queen Maud Land (SNA, NVL, SYO) also give negative residuals for the few events reported by them.

The average epicenter as located by ISC lies in a distance  $\Delta = 1417 \pm 25$  km from GvN. The observed travel-time corresponds to  $\Delta = 1370$  km, while the observed time difference between S and P phases results in a  $\Delta = 1314$  km.

Rather than assuming an abnormally high wave velocity somewhere on the wave path, it seems plausible to expect ISC-locations to be systematically biased in this region, especially since they are bound to depend heavily on South-American readings. Wavepaths towards South-America, however, transverse the high velocity subduction zone associated with the South-Sandwich islands. If this is not taken into consideration the mislocation will be such that negative residuals result at GvN. South-Sandwich events will be a preferred object of study in GvN-seismology in the future.

### 2. The Antarctic continent is not totally aseismic, but no local tectonic activity could be observed near GvN during a period of eight months

The low level of Antarctic seismicity has been an open question ever since the International Geophysical Year, especially because intraplate seismicity could give some clues to geological structure of an otherwise rather inaccessible continent (SYKES 1978). A few earthquakes have, however, been located in Antarctica (see WÜSTER 1989 for a map and a complete list) and even fewer with high certainty (ADAMS 1988). Three of these events could also be recorded at GvN (ECKSTALLER 1988, Figs. 5.1 and 5.2).

According to the empirical relationship between magnitude of earthquakes and their frequency of occurrence the number of earthquakes increases 3-fold to 30-fold for every unit of magnitude descended, depending on tectonic conditions. If this is true for Antarctica as well, tectonic microearthquakes should be discovered everywhere on this continent, too, provided magnification is sufficiently high. During 10 months in 1973, KAMINUMA (1976) observed 8 events with magnitudes between 0 and 1 near Syowa station. Data from the GvN network from October 1986 till June 1987 were carefully scrutinized, using all available methods described above, but not a single local tectonic event could be identified. Frequent periods of high noise level and/or instrumental malfunctioning cause gaps and leave enough room for speculation as yet. Data from the new remote stations on the southern ice-rises will help to clarify this question.

### 3. S-phases indicate a sedimentary sea-floor

S-phases can be identified in a few recordings (Fig. 8.). Their apparent velocities were determined with methods described above using data from the season 1986/87. This is generally not simple, because amplitudes are low and onset times are therefore difficult to pick. But, 5 out of 6 velocities obtained for the earthquake series mentioned above are definitely below the  $v_{app} = 4.6$  km/s derived from travel-time tables. In fact, velocities are in better agreement with the ice velocities  $v_p = 3.2 \dots 3.7$  and  $v_s = 1.6 \dots 1.9$  given by Eckstaller (1988). It can be concluded, that the S-phases observed are not SV/P-converted phases, but that they enter the ice at the ice-rises only, where there is no water to penetrate, and propagate horizontally along the ice-shelf.

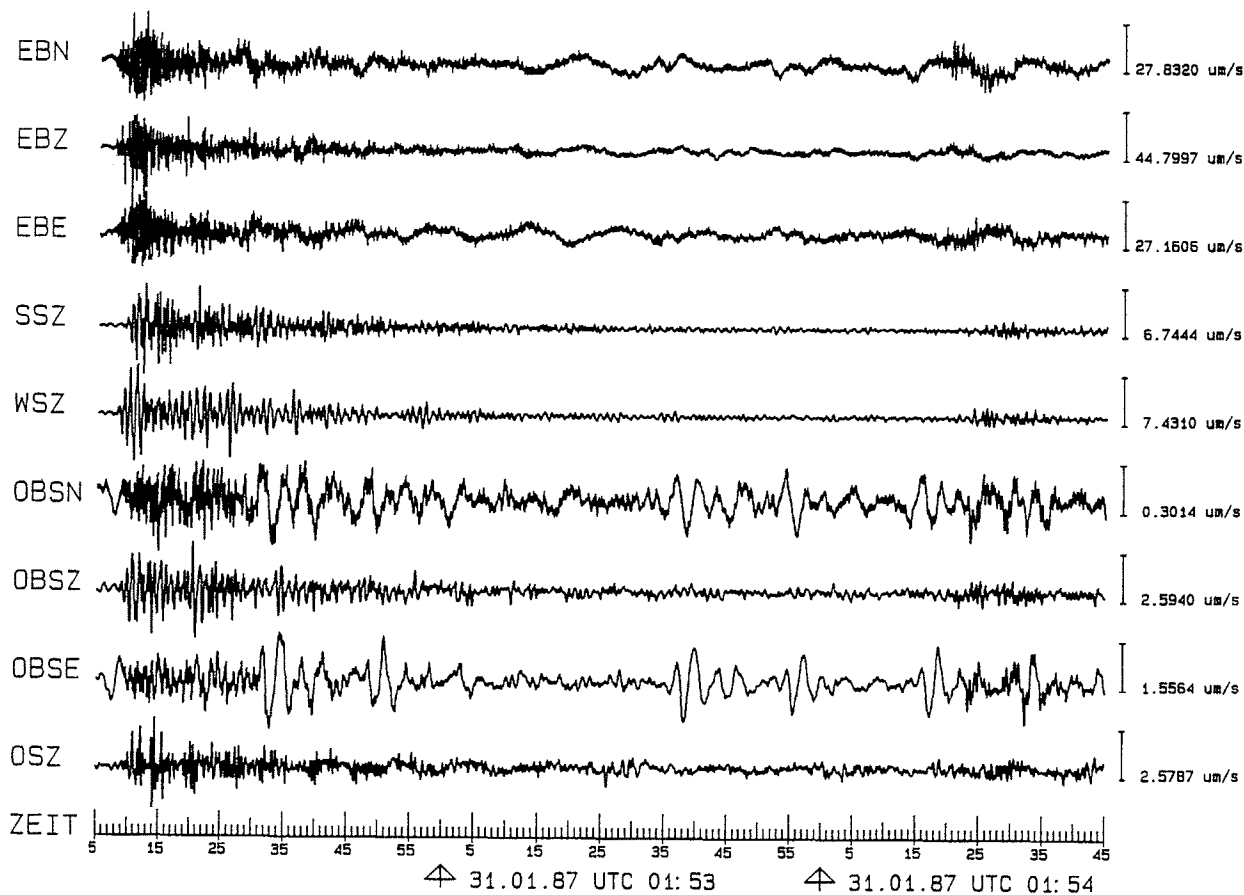


**Fig. 8:** One of the strongest aftershocks in earthquake-sequence on Jan. 30./31. 1987, recorded by the GvN network. Note the relatively slow resonances in the P wavetrain on WSz and OBSz as opposed to the high frequency signal at EBz. The very long rolling waves on horizontal components of EB are low mode icewaves not detected by short period seismometers. Prominent impulsive events on the horizontal component of station OBS probably represent the noise of an ice-floe „knocking“ at the shelf-ice. Approx. 130 s after the P-onset,  $\tilde{S}$ -phases (see text) can be found on all channels.

**Abb. 8:** Eines der stärksten Nachbeben der Bebenserie vom 30./31. Jan. 1987, aufgezeichnet vom GvN-Netzwerk. Interessant sind die relativ langsamen Resonanzen im P-Wellenzug an WSz und OBSz im Gegensatz zu dem hochfrequenten Signal an EBz. Die sehr langen, rollenden Wellen auf den Horizontalkomponenten von EB sind niedrige Moden von Eiswellen, die von kurzperiodischen Seismometern nicht registriert werden. Die auffälligen Auslenkungen an den Horizontalkomponenten von OBSz rühren wahrscheinlich von Eisschollen her, die gegen das Schelfeis „klopfen“. Ca. 130 sec nach dem P-Einsatz lassen sich  $\tilde{S}$ -Phasen (siehe Text) auf allen Kanälen beobachten.

These phases are termed  $\sim S$ . Their wave fronts are not quasi-planar at receiver distances, making calculation of  $v_{app}$  difficult.

Because of their higher apparent velocity, SV/P-converted phases should arrive earlier than the  $\sim S$ -phases. The fact, that they are not observed is a further indicator for an acoustically soft sea-floor (i.e. the existence of a sedimentary layer) below the ice-shelf.

#### 4. Suggesting an underground model for GvN

Not much is known with certainty about the earth's structure below GvN. Ice thicknesses have been probed with EMR-measurements and in a small seismic survey, which also supplied depths to the sea floor in some places and one zero-offset-time to the next discontinuity "U9" suggested by HINZ & KRISTOFFERSEN (1987). Below this discontinuity we expect volcanic and volcanoclastic sediments like in the so-called Explora Wedge identified by marine seismic surveys off the coast, with a thickness of 5 km to the basement (HINZ & KRISTOFFER-

SEN 1987). The structure of the intermeditate and lower crust appears fairly regular in refraction-seismic surveys on Queen Maud Land (ECKSTALLER et al. 1991). The mantle is assumed to resemble a model derived for East Antarctica (MCMECHAN 1981). Table 1 combines all these results and lists the sources.

From many optimizations in the calculation of apparent velocity  $v_{app}$  in the GvN network for a number of well-recorded earthquakes, a residual correction term for remote station EB of  $+0.25 \pm 0.05$  s has been obtained, which means that onsets arrive on the average 0.25 s earlier at EB than they should if the structure of the deeper earth is laterally homogeneous over the width of the network. It is known that the ice-shelf rests on a rise in the sea floor at EB, producing the ice rumple to the north-east of the base. The simplest assumption is, that here the sea-floor consists of the material of the layer below the discontinuity U9 with a  $v_p = 4.5$  km/s rather than of sediments with average  $v_p = 2.5$  km/s. A schematic 2-dimensional model is depicted in Figure 10. A calculation of travel time differences for the rays shown indeed yields a negative residual for EB. A theoretical

station correction term needed to make up for this residual is  $\Delta_{EB} = +0.29$  s for epicenters in the South-Sandwich area ( $\Delta = 13^\circ$ ) and  $\Delta_{EB} = +0.33$  s for epicenters near Vanuatu ( $\Delta = 95^\circ$ ). This is a good match for the experimentally found station correction term, adding some credibility to the model. Further adjustments to the model cannot be justified by a single value, but here lies the beginning of seismic tomography.

## CONCLUSIONS

GvN base has proven its usefulness as a site for seismological research, in spite of the obvious disadvantage of its setting on a floating ice-shelf. Apart from contributing to the world-wide network of seismograph stations, data from GvN have been used in specialized studies focusing on icequakes, local seismicity and anomalies of seismic velocities within the earth's crust and upper mantle. Future research interest will concentrate on South-

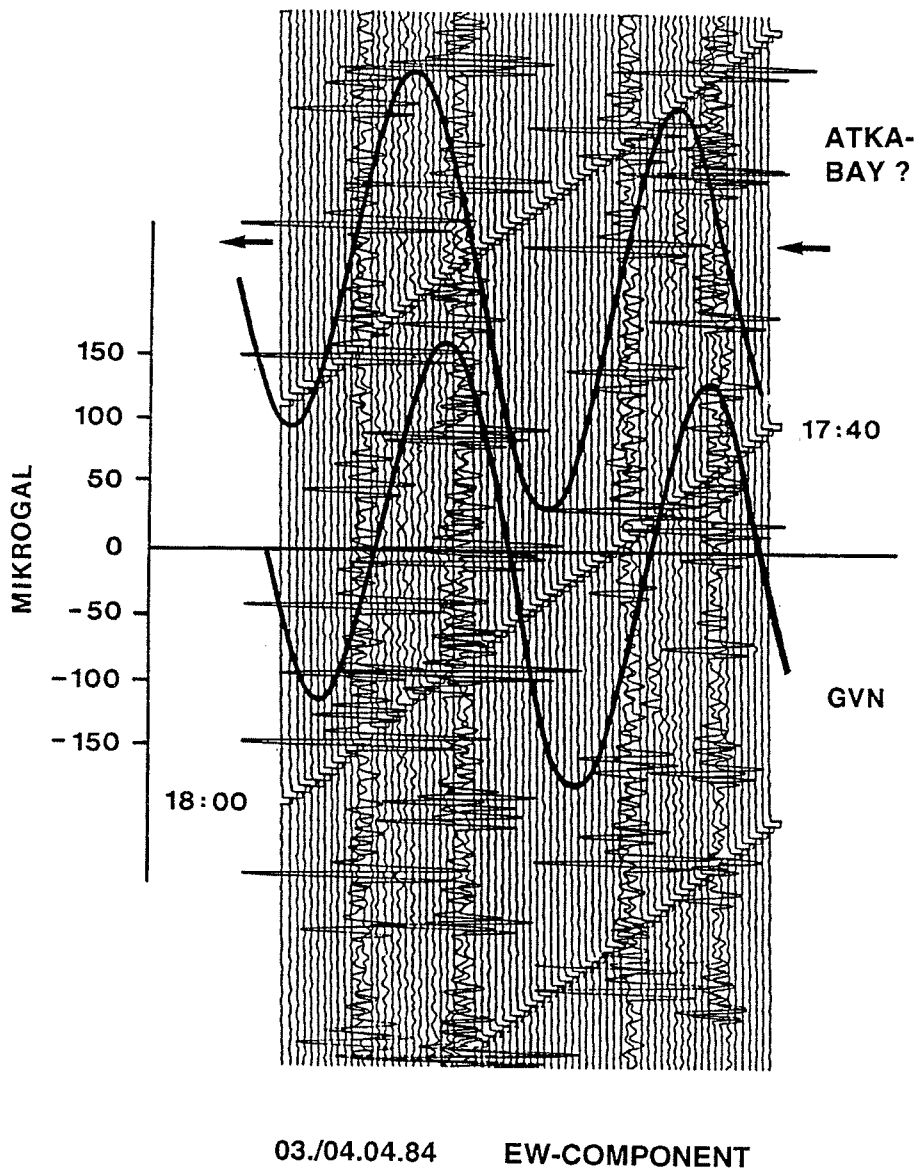


**Fig. 9:** This special type of ground noise recorded on EW-component at seismic station OBS is interpreted as a series of impacts exerted on the ice-shelf by ice-floes drifting in tidal currents in neighbouring Atka Bay. The lower curve drawn across the seismogram represents the tidal gravity anomaly measured at GvN. If this curve is shifted by approx. 1 hour to the left (upper curve), the zeroes of the anomaly - corresponding to maximum tidal current - coincide with the bands of increased noise. This indicates a phase shift of tidal movements between GvN and Atka Bay.

**Abb. 9:** Diese besondere Art von Störsignal, registriert auf der EW-Komponente von OBS wird als Serie horizontaler Schläge interpretiert, den in der benachbarten Atka-Bucht treibende Eisschollen im Rhythmus des Seegangs auf das Schelfeis ausüben. Die unten quer über das Seismogramm aufgetragene Kurve zeigt den an GvN gemessenen Gezeitengang der Schwere. Wenn diese Kurve um etwa 1 Stunde nach links verschoben wird (obere Kurve), dann fallen die Nulldurchgänge der Gezeitenströmung, entsprechend dem Maximum des Gezeitenstroms, mit den Bändern starker Störsignale zusammen. Es zeigt sich eine Phasenverschiebung der Gezeitenströmung zwischen GvN und der Atka-Bucht.

Tab. 1: Review of surveys with relevance for crustal structure below GvN (1-dimensional model).

Tab. 1: Zusammenfassung der Untersuchungsergebnisse mit Relevanz für die Krustenstruktur unter GvN (eindimensionales Modell).

discont.	depth (km)	layer	thickness (km)	$v_p$ (km/s)	reference
surface	0.04				
		shelf ice	0.21	3.70	HOYER (1983) ECKSTALLER (1988)
ice edge	-0.17				
		sea water	0.11	1.44	HOYER (1983)
sea floor	-0.28				
		sediment	1.55	2.52	HINZ & KRISTOFFERSEN (1987)
U9	-1.83				
		Explora Wedge	5.0	4.5	HINZ et al. (1987) HINZ & KRISTOFFERSEN (1987) $v_p$ : KAUL (pers. comm.)
basement	-6.83				
		1 <sup>st</sup> crustal layer		6.3 (6.0)	IKAMI & ITO (1986)
	-15.3 (-9.5)	2 <sup>nd</sup> crustal layer		6.6 (6.2)	IKAMI & ITO (1986)
Conrad	-31.0 (-16.9)	lower crust		6.8 (6.76)	KOGAN (1970)
Moho	-42.0 (-38.0)	upper mantle		7.9	
	-111.0	mantel		8.5	MCMECHAN (1981)

Sandwich events, on crustal transfer functions and on possible shear wave splitting due to the expected anisotropy.

#### ACKNOWLEDGMENT

We want to thank all geophysicists, A. Brodscholl, K. Wallner, W. Kobarg, E. Lippmann, C. Walter, H. v. d. Osten-Woldenburg, N. Kaul, A. Unterschütz, U. Nixdorf, S. Reiprich, O. Andresen, A. Steffen, S. Brylka, M. Lang, M. Sobiesiak, E. Weigelt, C. Mayer, K. Mühlstein, who have wintered at Georg-von-Neumayer base in these nine seasons. Without their continuous labour there would be no data.

#### References

- Adams, R.D. (1988): Antarctic earthquakes.- Nature 331: 665.
- Eckstaller, A. (1988): Seismologische Untersuchungen mit Daten der Georg-von-Neumayer-Station, Antarktis.- Unpubl. Dissertation, University München.
- Eckstaller, A., Brodscholl, A., Mandler, H., Miller, G. Nixdorf, U., Patzelt, G., Pietschmann, M. & Rott, H.: (1991) Refraktionsseismik. in: H. Miller & H. Oerter (eds.): Die Expedition ANTARKTIS-VIII mit FS „Polarstern“ 1989/90. Berichte Polarforsch. 86: 108-115.
- Hatherton, T. (1961): A note on the seismicity of the Ross Sea Region.- Geophys. J. R. Astron. Soc. 5: 252-253.
- Hinz, K. & Kristofferson, Y. (1987): Antarctica: recent advances in the understanding of the continental shelf.- Geol. Jb. E37: 3-64.
- Ikami, A. & Ito, K. (1984): Nature of noises on ice sheet in East Antarctica.- Nat. Inst. Polar Res., Mem. Ser.C15: 43-60.
- Kaminuma, K. (1976): Seismicity in Antarctica.- J. Phys. Earth 24: 381-395.
- Kobarg, W. & Lippmann, E. (1986): Gezeitenmessungen auf dem Ekström-Schelfeis, Antarktis.- Polarforschung 56: 1-21.
- McMechan, G. (1981): Mantle P-wave velocity structure beneath Antarctica.- Bull. Seism. Soc. Am. 71: 1061-1074.
- Miller, H. & Eckstaller, A. (1982): Das geophysikalische Observatorium an der Georg-von-Neumayer-Station.- Berichte Polarforsch. 6: 43-49.
- Miller, H., Brodscholl, A. & Wallner, K. (1983): Sommerkampagne 1982/83 Gruppe Geophysik.- Berichte Polarforsch. 13: 67-70.
- Mühlstein K. (1990): Reflektions- und Refraktionsseismische Bearbeitung von Daten aus dem Ekström-Schelfeis unter besonderer Berücksichtigung der Schichtgrenzen von Eis zum nächsten Medium.- Unpubl. Ber. Inst. Geophysik TU Clausthal.

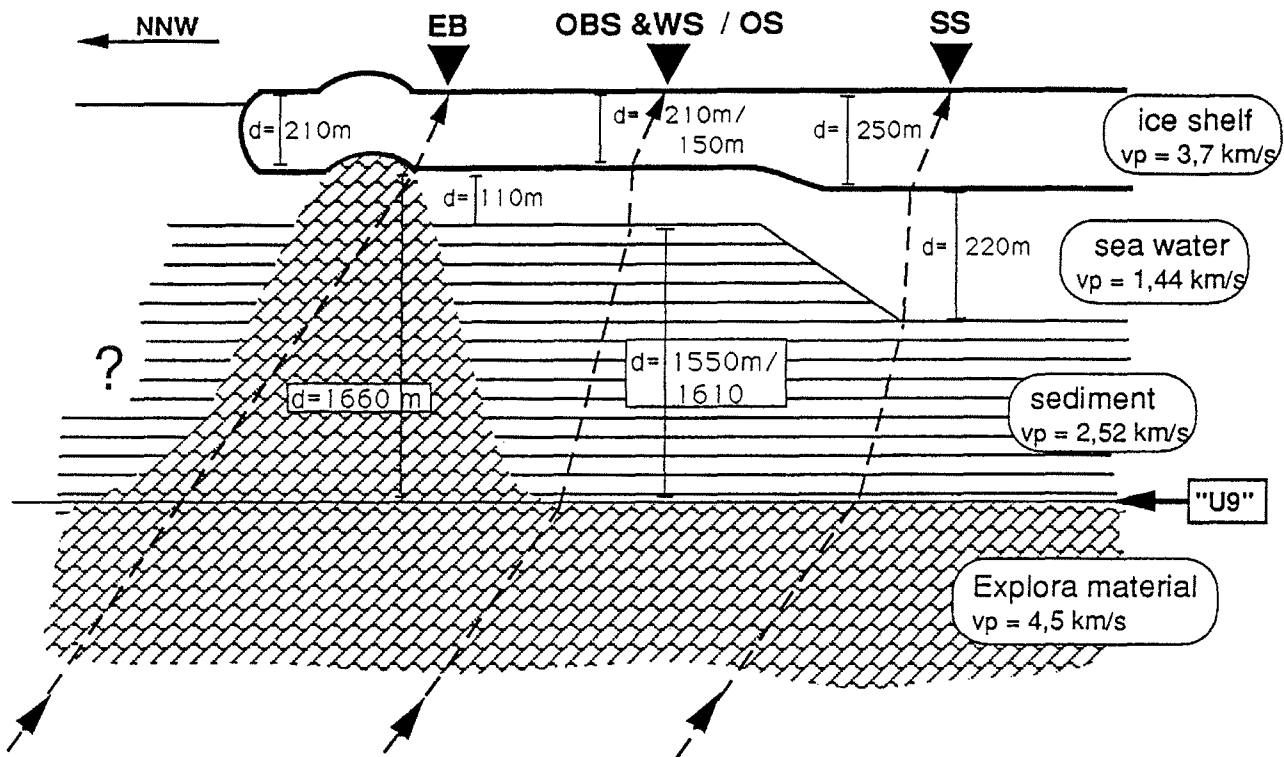


**Fig. 10:** Schematic view of (2-dimensional) underground model proposed for GvN (not to scale.) Seismic stations are depicted by black triangles, thicknesses are denoted by  $d$  and p-wave velocities by  $v_p$ . The model is based on previous studies mentioned in Fig. 9. It is constrained by local travel time anomalies observed across the seismic network around GvN. Ray paths are depicted as broken lines with arrows.

**Abb. 10:** Zweidimensionales, schematisches Untergrundmodell, das für GvN vorgeschlagen wird (nicht maßstabsgetreu). Schwarze Dreiecke repräsentieren seismische Stationen, Schichtdicken sind mit  $d$  und seismische Geschwindigkeiten mit  $v_p$  bezeichnet. Das Modell beruht auf früheren Untersuchungen (siehe Abb. 9) und wird durch lokale Laufzeitresiduen zwischen den Stationen des GvN-Netzes eingegrenzt. Strahllaufwege sind als gestrichelte Linien mit Pfeilen abgebildet:

*Nishio, F.* (1983): Studies on thermally induced fractures and snowquakes of polar snow cover.- Nat. Inst. Polar Res., Memoirs Ser.C14.

*Nixdorf, U.* (1992): Dehnungsbeben in einer Störungszone im Ekström-Schelfeis nördlich der Georg-von-Neumayer-Station, Antarktis - eine Untersuchung mit seismologischen und geodätischen Methoden.- Berichte Polarforsch. 108: 1-101.

*Wüster, J.* (1989): Suche nach lokaler Seismizität mit dem kurzperiodischen Seismographennetz um die Georg-von-Neumayer-Station, Antarktis.- Unpubl. Diplomarbeit Univ. Bremen.

*v.d. Osten-Woldenburg, H.* (1990): Icequakes on Ekström ice shelf near Atka Bay, Antarktica.- J. Glaciology 36/122: 31-36.